

P -wave coupled channel effects in electron-positron annihilation

Meng-Lin Du,^{1,*} Ulf-G. Meißner,^{1,2,†} and Qian Wang^{1,‡}

¹*Helmholtz-Institut für Strahlen- und Kernphysik and Bethe Center for Theoretical Physics,
Universität Bonn, D-53115 Bonn, Germany*

²*Institut für Kernphysik, Institute for Advanced Simulation, and Jülich Center for Hadron Physics,
D-52425 Jülich, Germany*

P -wave coupled channel effects arising from the $D\bar{D}$, $D\bar{D}^* + c.c.$, and $D^*\bar{D}^*$ thresholds in e^+e^- annihilations are systematically studied. We provide an exploratory study by solving the Lippmann-Schwinger equation with short-ranged contact potentials obtained in the heavy quark limit. These contact potentials can be extracted from the P -wave interactions in the e^+e^- annihilations, and then be employed to investigate possible isosinglet P -wave hadronic molecules. In particular, such an investigation may provide information about exotic candidates with quantum numbers $J^{PC} = 1^{-+}$. In the mass region of the $D\bar{D}$, $D\bar{D}^* + c.c.$, and $D^*\bar{D}^*$ thresholds, there are two quark model bare states, i.e. the $\psi(3770)$ and $\psi(4040)$, which are assigned as (1^3D_1) and (3^1S_1) states, respectively. By an overall fit of the cross sections of $e^+e^- \rightarrow D\bar{D}$, $D\bar{D}^* + c.c.$, $D^*\bar{D}^*$, we determine the physical coupling constants to each channel and extract the pole positions of the $\psi(3770)$ and $\psi(4040)$. The deviation of the ratios from that in the heavy quark spin symmetry (HQSS) limit reflects the HQSS breaking effect due to the mass splitting between the D and the D^* . Besides the two poles, we also find a pole a few MeV above the $D\bar{D}^* + c.c.$ threshold which can be related to the so-called $G(3900)$ observed earlier by BABAR and Belle. This scenario can be further scrutinized by measuring the angular distribution in the $D^*\bar{D}^*$ channel with high luminosity experiments.

PACS numbers: 14.40.Pq, 11.55.Bq, 12.38.Lg, 14.40.Rt

I. INTRODUCTION

Since the observation of the $X(3872)$ in 2003, numerous exotic candidates which do not fit into the conventional quark model spectrum have been observed in experiments. Most of these exotic candidates appear near some open-flavor thresholds which calls for a systematical study of the threshold or coupled channel effects in the relevant channels. For the S -wave interaction, the most famous one is $D\bar{D}^*$ interaction in the isospin singlet channel which is crucial for understanding the nature of the $X(3872)$ [1–9]. The corresponding coupled channel effects in the isovector channel have also been studied to probe the structure of the $Z_c(3900)$ and the $Z_c(4040/4025)$ [10–18] as well as their heavy flavor partners in the bottom sector, i.e. $Z_b(10610)$ and $Z_b(10650)$ [19–23], which are close to the $B\bar{B}^*$ and $B^*\bar{B}^*$ thresholds, respectively. Since the S -wave interaction among hadrons can form a bound state more easily than other partial waves, the nearby S -wave threshold and the S -wave interaction which might form a hadronic molecule have attracted a lot of attention. Although an interaction in higher partial waves cannot easily form a bound state, it could also have moderate effects on certain observables within the relevant energy region, especially the next alternative option of a P -wave. Besides the potential S -wave hadronic molecules mentioned above, there are also some vector exotic candidates which appear in e^+e^- annihilation, such as $G(3900)$ [24, 25], $Y(4008)$ [26], $Y(4260)$ [27], $Y(4360)$ [28], $Y(4630)$ [29], $Y(4660)$ [30, 31] and so on.

With the availability of high-luminosity data from Belle and BESIII for e^+e^- annihilation, it is timely to study the P -wave interactions between a pair of S -wave heavy-light mesons, such as $D\bar{D}$, $D\bar{D}^*$, and $D^*\bar{D}^*$, as well as the S -wave interactions between one S -wave heavy-light meson and one P -wave heavy-light meson, such as $D_1\bar{D} + c.c.$, $D_1\bar{D}^* + c.c.$, and $D_2\bar{D}^* + c.c.$ pairs. This will help

*Electronic address: du@hiskp.uni-bonn.de

†Electronic address: meissner@hiskp.uni-bonn.de

‡Electronic address: wangqian@hiskp.uni-bonn.de

¹ Here and in what follows, $D\bar{D}^*$ means $D\bar{D}^* + c.c.$ which includes its charged conjugate partner to form a C -parity eigenstate.

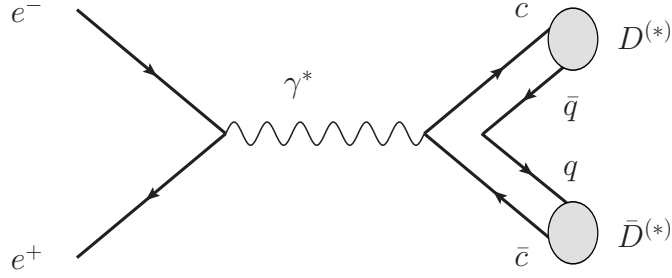


FIG. 1: Feynman diagram for e^+e^- to a pair of charmed mesons.

us understand both the conventional heavy quarkonium and the vector exotic candidates. Since in the heavy quark limit the interaction between the two spin multiplets share the same low-energy parameters, the study will also shed light on the existence of other possible exotic candidates but with different quantum numbers. However, up to now, most of the studies on the P -wave or S -wave threshold effect in e^+e^- colliders are mainly based on the one-loop calculation [32–37] within some power counting schemes [38] or the effective Lagrangian approach. There are also some studies [39–42] which focus on the one-channel case. As a result, a systematic study of the P -wave as well as the S -wave interaction in e^+e^- annihilation is called for.

In this paper, we study the P -wave $D\bar{D}$, $D\bar{D}^*$, and $D^*\bar{D}^*$ (Fig. 1) coupled channel effects in e^+e^- annihilation within the energy region [3.70, 4.25] GeV. Since the probability for the creation of a pair of strange quarks is much smaller than that of an up and/or down quark pair, we neglect the strange charmed thresholds.² The next open flavor channel should be included, such as $D_1\bar{D}$ (about 4.29 GeV), as long as the energy exceeds the production threshold. This is the reason why we only consider the energy below 4.25 GeV. As we are performing an exploratory study, we include the short-ranged contact potential in the heavy quark limit in addition to the conventional charmonia without including the one-pion exchanged potential.³ In Sec. II, we present the decomposition of P -wave heavy-light meson pair in the heavy quark limit and the corresponding Lippmann-Schwinger equation. Section III contains the results and discussion. We end with a summary in Sec. IV.

II. FORMALISM

In this section, we present the decomposition formula of the P -wave $D\bar{D}$, $D\bar{D}^*$, and $D^*\bar{D}^*$ with quantum number $J^{PC} = 1^{--}$ in terms of the heavy and light degrees of freedom which are conserved, respectively, in the heavy quark limit. Accordingly, the short-ranged contact potentials can be obtained from this decomposition. In what follows, the Lippmann-Schwinger equation in the calculation is presented explicitly.

² A further argument in favor of this assumption is the fact that the cross section of $e^+e^- \rightarrow D_s^{(*)}\bar{D}_s^{(*)}$ [43] is about one order of magnitude smaller than those of $e^+e^- \rightarrow D\bar{D}$, $D\bar{D}^*$, and $D^*\bar{D}^*$.

³ The discussion of the one-pion exchange potential and the relevant three-body channels, such as $D\bar{D}\pi$, $D\bar{D}^*\pi$ will be included in the forthcoming work as well as the next S -wave thresholds, i.e. $D_1\bar{D} + c.c.$, $D_1\bar{D}^* + c.c.$, and $D_2\bar{D}^* + c.c.$.

TABLE I: The relative partial widths of a S -wave and a D -wave charmonium to a pair of charmed mesons. The subscripts are the total spin of the two charmed meson system.

Charmonium	$ D\bar{D}\rangle_0$	$ D^*\bar{D}\rangle_1$	$ D\bar{D}^*\rangle_1$	$ D^*\bar{D}^*\rangle_0$	$ D^*\bar{D}^*\rangle_1$	$ D^*\bar{D}^*\rangle_2$
S -wave	$\frac{1}{12}$	$\frac{1}{6}$	$\frac{1}{6}$	$\frac{1}{36}$	0	$\frac{5}{9}$
D -wave	$\frac{5}{12}$	$\frac{5}{24}$	$\frac{5}{24}$	$\frac{5}{36}$	0	$\frac{1}{36}$

A. Decomposition of P -wave $D\bar{D}$, $D\bar{D}^*$, and $D^*\bar{D}^*$ pairs

The decomposition of a pair of charmed mesons with a relative orbital angular momentum l reads⁴

$$|l([s_{l_1}s_{Q_1}]_{j_1}[s_{l_2}s_{Q_2}]_{j_2})_s\rangle_J = \sum_{s_l, s_Q, s_q} (-1)^{l+s_q+s_Q+J} \hat{s}_q \hat{s}_Q \hat{j}_1 \hat{j}_2 \hat{s} \hat{s}_l \begin{Bmatrix} s_{l_1} & s_{Q_1} & j_1 \\ s_{l_2} & s_{Q_2} & j_2 \\ s_q & s_Q & s \end{Bmatrix} \times \begin{Bmatrix} l & s_q & s_l \\ s_Q & J & s \end{Bmatrix} |(l[s_{l_1}s_{l_2}]_{s_q})_{s_l}[s_{Q_1}s_{Q_2}]_{s_Q}\rangle_J, \quad (1)$$

where $|l([s_{l_1}s_{Q_1}]_{j_1}[s_{l_2}s_{Q_2}]_{j_2})_s\rangle_J$ is the hadronic basis with s_{Q_i} and s_{l_i} the heavy quark spin and the spin plus relative orbital angular momentum of the light degrees of freedom in the i th hadron, respectively, j_i is the spin of the i th hadron and s is the sum of them. Further, l and J are the relative orbital angular momentum and total angular momentum of the two-hadron system, respectively. The hadronic basis can be reexpressed as Eq. (1) in terms of the heavy and light degrees of freedom basis $|(l[s_{l_1}s_{l_2}]_{s_q})_{s_l}[s_{Q_1}s_{Q_2}]_{s_Q}\rangle_J$, with s_Q the total spin of the heavy quark pair, s_q is the total spin of the light degrees of freedom, and s_l their total spin plus relative orbital angular momentum, $s_l = s_q + l$. Since s_Q and s_l are conserved, respectively, in the heavy quark spin symmetry (HQSS) limit, $|(l[s_{l_1}s_{l_2}]_{s_q})_{s_l}[s_{Q_1}s_{Q_2}]_{s_Q}\rangle_J$ can be simplified as $|s_Q \otimes s_l\rangle_J$. Using Eq. (1), one can obtain the decompositions of the P -wave charmed meson pair with $J^{PC} = 1^{--}$ as [44]

$$|D\bar{D}\rangle_{1^{--}} = \frac{1}{2}|0 \otimes 1\rangle + \frac{1}{2\sqrt{3}}|1 \otimes 0\rangle - \frac{1}{2}|1 \otimes 1\rangle + \frac{1}{2}\sqrt{\frac{5}{3}}|1 \otimes 2\rangle, \quad (2)$$

$$|D\bar{D}^* + c.c.\rangle_{1^{--}} = -\frac{1}{\sqrt{3}}|1 \otimes 0\rangle + \frac{1}{2}|1 \otimes 1\rangle + \frac{1}{2}\sqrt{\frac{5}{3}}|1 \otimes 2\rangle, \quad (3)$$

$$|D^*\bar{D}^*\rangle_{1^{--}}^{s=0} = \frac{1}{2}\sqrt{3}|0 \otimes 1\rangle - \frac{1}{6}|1 \otimes 0\rangle + \frac{1}{2\sqrt{3}}|1 \otimes 1\rangle - \frac{\sqrt{5}}{6}|1 \otimes 2\rangle, \quad (4)$$

$$|D^*\bar{D}^*\rangle_{1^{--}}^{s=2} = \frac{\sqrt{5}}{3}|1 \otimes 0\rangle + \frac{1}{2}\sqrt{\frac{5}{3}}|1 \otimes 1\rangle + \frac{1}{6}|1 \otimes 2\rangle. \quad (5)$$

These wave functions are normalized to one and orthogonal to each other. The coefficients can be written as a compact matrix

$$g^{1^{--}} = \begin{pmatrix} \frac{1}{2} & \frac{1}{2\sqrt{3}} & -\frac{1}{2} & \frac{1}{2}\sqrt{\frac{5}{3}} \\ 0 & -\frac{1}{\sqrt{3}} & \frac{1}{2} & \frac{1}{2}\sqrt{\frac{5}{3}} \\ \frac{1}{2}\sqrt{3} & -\frac{1}{6} & \frac{1}{2\sqrt{3}} & -\frac{\sqrt{5}}{6} \\ 0 & \frac{\sqrt{5}}{3} & \frac{1}{2}\sqrt{\frac{5}{3}} & \frac{1}{6} \end{pmatrix}. \quad (6)$$

⁴ Here $\hat{j} = \sqrt{2j+1}$.

As a by-product, pairs with a possible exotic quantum number can also be obtained:

$$|D\bar{D}^* + c.c.\rangle_{1-+} = -\frac{1}{\sqrt{2}}|0 \otimes 1\rangle + \frac{1}{\sqrt{2}}|1 \otimes 1\rangle, \quad (7)$$

$$|D^*\bar{D}^*\rangle_{1-+}^{s=1} = \frac{1}{\sqrt{2}}|0 \otimes 1\rangle + \frac{1}{\sqrt{2}}|1 \otimes 1\rangle. \quad (8)$$

In the heavy quark limit, the S -wave and D -wave charmonia couple to a pair of charmed mesons through the $|1 \otimes 0\rangle$ and $|1 \otimes 2\rangle$ components, respectively. Therefore, their decay widths are proportional to the corresponding Clebsch-Gordan coefficient squared.⁵ The relative branching ratios are listed in Table I.⁶ This relation can also be obtained by constructing the effective interaction based on HQSS as shown in Appendix A.

In the heavy quark limit, we can define the direct contact potentials

$$C_1 \equiv V_{01} = \langle 0 \otimes 1 | \hat{H} | 0 \otimes 1 \rangle, \quad C_2 \equiv V_{10} = \langle 1 \otimes 0 | \hat{H} | 1 \otimes 0 \rangle, \quad (9)$$

$$C_3 \equiv V_{11} = \langle 1 \otimes 1 | \hat{H} | 1 \otimes 1 \rangle, \quad C_4 \equiv V_{12} = \langle 1 \otimes 2 | \hat{H} | 1 \otimes 2 \rangle, \quad (10)$$

which are considered as constant within the small energy region we consider. Besides the four open charm channels, i.e. the $D\bar{D}$, $D\bar{D}^* + c.c.$, $D^*\bar{D}_{s=0}^*$, and $D^*\bar{D}_{s=2}^*$ channels, there are also four expected conventional charmonia within this region, i.e. $\psi(2S)$, $\psi(1D)$, $\psi(3S)$, $\psi(2D)$. In the following, we use the latin letters $i, j, \dots = 1, 2, 3, 4$ to denote the open charm channels and the greek letters $\alpha, \beta, \dots = 1, 2, 3, 4$ to denote the bare pole terms. As a result, the corresponding potential among these eight channels is

$$V = \begin{pmatrix} v_{ij} & v_{i\beta} \\ v_{\alpha j} & 0 \end{pmatrix} \quad (11)$$

with

$$v_{ij} = g_{ik}^{1--} g_{jk}^{1--} C_k, \quad v_{i\beta} = g_{i\ell}^{1--} \mu_{\ell\beta}, \quad v_{\alpha j} = g_{jk}^{1--} \mu_{k\alpha}.$$

Here, $\mu_{\beta l} = \mu_{l\beta} \neq 0$ only when $\beta = 1, 3$, and $l = 2$ or $\beta = 2, 4$ and $l = 4$. For further use, we rename the coupling constants

$$\mu_{21} \equiv g_{2S}, \quad \mu_{23} \equiv g_{3S}, \quad \mu_{42} \equiv g_{1D}, \quad \mu_{44} \equiv g_{2D}, \quad (12)$$

so that their physical meanings are manifest, i.e. these are the couplings between the bare charmonia and the open charmed channels.

B. The Lippmann-Schwinger equation

Due to the zero component in Eq.(11), the Lippmann-Schwinger equation (LSE), $T = V - VGT$, can be split into two subgroups

$$T_{ij} = V_{ij} - V_{ik} G_k T_{kj} - V_{i\alpha} S_\alpha T_{\alpha j}, \quad (13)$$

$$T_{\alpha i} = V_{\alpha i} - V_{\alpha j} G_j T_{ji}, \quad (14)$$

and

$$T_{i\alpha} = V_{i\alpha} - V_{ij} G_j T_{j\alpha} - V_{i\beta} S_\beta T_{\beta\alpha}, \quad (15)$$

$$T_{\alpha\beta} = -V_{\alpha i} G_i T_{i\beta}, \quad (16)$$

⁵ In the energy region where $\psi(nS)$ dominates, the ratio of the cross sections $e^+e^- \rightarrow D\bar{D}$, $D\bar{D}^* + c.c.$, $D^*\bar{D}_{s=0}^*$ and $D^*\bar{D}_{s=2}^*$ is also consistent with the ratio for the S -wave charmonium given in Table I in the HQSS limit.

⁶ One should notice that the ratios are obtained in the heavy quark limit which means the masses of D and D^* are equal to each other. In this case, the phase space factors of the different channels are the same and will thus not modify these ratios.

with G_i the two-body propagator and $S_\alpha = (m_\alpha^2 - s)^{-1}$ the bare pole propagator. Substituting Eq. (14) into Eq. (13), one can obtain

$$T_{ij} = \hat{V}_{ij} - \hat{V}_{ik} G_k T_{kj} \quad (17)$$

with the effective potential $\hat{V}_{ij} = V_{ij} - V_{i\alpha} S_\alpha V_{\alpha j}$. With the above equation for T_{ij} and Eq. (14), one can also calculate the transition matrix $T_{\alpha i}$ between the charmonia and the charmed meson pair. Substituting Eq. (16) into Eq. (15), one can also extract the transition matrix from bare charmonia to the open charmed channels

$$T_{i\alpha} = V_{i\alpha} - \hat{V}_{ij} G_j T_{j\alpha} . \quad (18)$$

Again, the transition matrix $T_{\alpha\beta}$ among the charmonia can be extracted from Eq. (16) accordingly. Now the 8×8 matrix is reduced to several 4×4 matrices.

The bare production amplitude is defined as

$$\mathcal{F} = (F_1, F_2, F_3, F_4, f_1, f_2, f_3, f_4)^T$$

with $f_1 \equiv g_{2S}^0$, $f_2 \equiv g_{1D}^0$, $f_3 \equiv g_{3S}^0$, $f_4 \equiv g_{2D}^0$ the couplings between the virtual photon and the corresponding charmonia. $F_i \equiv g_{i2}^{1--} f_S^0 + g_{i4}^{1--} f_D^0$ is the coupling between the virtual photon and the i th open charmed channel. The physical production amplitude can be obtained from

$$\mathcal{U} = \mathcal{F} - V G \mathcal{U} ,$$

with the physical production amplitudes of the open charm channels and bare poles given by

$$\mathcal{U}_i = \mathcal{F}_i - V_{ij} G_j \mathcal{U}_j - V_{i\alpha} S_\alpha \mathcal{U}_\alpha , \quad (19)$$

$$\mathcal{U}_\alpha = f_\alpha - V_{\alpha j} G_j \mathcal{U}_j . \quad (20)$$

Substituting Eq.(20) to Eq.(19), one can obtain the physical production amplitudes of the open charm channels

$$\mathcal{U}_i = \mathcal{F}_i - V_{i\alpha} S_\alpha f_\alpha - V_{ij} G_j \mathcal{U}_j + V_{i\alpha} S_\alpha V_{\alpha j} G_j \mathcal{U}_j \quad (21)$$

$$= \hat{\mathcal{F}}_i - \hat{V}_{ij} G_j \mathcal{U}_j \quad (22)$$

in terms of the effective bare production amplitudes $\hat{\mathcal{F}}_i = \mathcal{F}_i - V_{i\alpha} S_\alpha f_\alpha$ and the effective potentials \hat{V}_{ij} . Here the contribution of the bare charmonium pole is absorbed into the definition of the effective bare production amplitudes $\hat{\mathcal{F}}_i$ and the effective potentials \hat{V}_{ij} .

Since we only consider separable contact potentials in our calculation, the momentum from the two P -wave vertices can be absorbed into the definition of the two-body propagator G_i as

$$G_{D\bar{D}}^{ij} = -4i \int \frac{d^4 l}{(2\pi)^4} \frac{l^i l^j}{(l^2 - m_1^2 + i\epsilon)((p-l)^2 - m_2^2 + i\epsilon)} , \quad (23)$$

$$G_{D\bar{D}^*}^{ij} = -4i \int \frac{d^4 l}{(2\pi)^4} \frac{\frac{1}{2} \varepsilon^{imn} \varepsilon^{jmk} l^n l^k}{(l^2 - m_1^2 + i\epsilon)((p-l)^2 - m_2^2 + i\epsilon)} , \quad (24)$$

$$G_{D^* \bar{D}^*_{s=0}}^{ij} = -4i \int \frac{d^4 l}{(2\pi)^4} \frac{l^i l^j}{(l^2 - m_1^2 + i\epsilon)((p-l)^2 - m_2^2 + i\epsilon)} , \quad (25)$$

$$G_{D^* \bar{D}^*_{s=2}}^{ij} = -4i \int \frac{d^4 l}{(2\pi)^4} \frac{P_2^{ik,mn} P_2^{jl,pq} \delta^{mp} \delta^{nq} l^k l^l}{(l^2 - m_1^2 + i\epsilon)((p-l)^2 - m_2^2 + i\epsilon)} , \quad (26)$$

with the $s = 0$ and $s = 2$ projectors

$$P_0^{ij} = \frac{1}{\sqrt{3}} \delta^{ij} , \quad P_2^{ij,mn} = \sqrt{\frac{3}{5}} \left(\frac{1}{2} \delta^{im} \delta^{jn} + \frac{1}{2} \delta^{in} \delta^{jm} - \frac{1}{3} \delta^{ij} \delta^{mn} \right) \quad (27)$$

for the $D^* \bar{D}^*$ channel. In principle, the two additional momentum factors from two P -wave vertices $l^\mu l^\nu$ can be reduced as $\mathcal{G}_{00} g^{\mu\nu} + p^\mu p^\nu \mathcal{G}_{11}$, with p the external momentum. Since the photon is produced from $e^+ e^-$ annihilation, it is transversely polarized, $-g^{\mu\nu} + \frac{p^\mu p^\nu}{p^2} \sim \delta^{ij}$, with i, j being spatial indexes. As a result, Eqs. (23)-(26) can be simplified as $-4\mathcal{G}_{00}(s, m_{i1}^2, m_{i2}^2)$, with m_{i1} and m_{i2} the masses of the i th channels and s the incoming energy squared, times the corresponding interaction structure. The definition of \mathcal{G}_{00} can be found in Appendix B.

C. The cross section

As shown in Fig.1, the scattering amplitude for the process $e^+e^- \rightarrow D^{(*)}\bar{D}^{(*)}$ is

$$\mathcal{M} = \bar{v}(p_+)(-ie\gamma_\mu)u(p_-)\frac{iP_\gamma^{\mu\nu}(p)}{s}\mathcal{T}_\nu \quad (28)$$

with p_- (p_+) the four-momentum of the electron (positron) and p the sum of them. $P_\gamma^{\mu\nu}(p) = -g^{\mu\nu}$ is the numerator of the photon propagator. As discussed in the above section, since the photon has a transversal polarization, only the transverse part $P_\gamma^{T\mu\nu}(p) = -g^{\mu\nu} + \frac{p^\mu p^\nu}{p^2}$ contributes. \mathcal{T}^ν is the production amplitude obtained from the LSE. Then the amplitude squared is

$$|\mathcal{M}|^2 = 4\frac{e^2}{s^2}\left(p_+^\nu p_-^{\nu'} + p_-^\nu p_+^{\nu'} - \frac{1}{2}sg^{\nu\nu'}\right)\mathcal{T}_\nu\mathcal{T}_{\nu'}^* \quad (29)$$

$$= 4\frac{e^2}{s^2}\left(\frac{1}{2}s\delta^{ij} - 2p_+^i p_+^j\right)\mathcal{T}^i\mathcal{T}^{*j} \quad (30)$$

with $s = p^2$. The production amplitudes for the four open charmed channels are

$$\mathcal{T}_1^i = \mathcal{U}_1(p_D^i - p_{D^*}^i), \quad (31)$$

$$\mathcal{T}_2^i = \mathcal{U}_2\epsilon^{ijk}(p_D^j - p_{D^*}^j)\epsilon^{*k}, \quad (32)$$

$$\mathcal{T}_3^i = \mathcal{U}_3\frac{1}{\sqrt{3}}(p_{D^*}^i - p_{D^*}^i)\epsilon_{D^*}^* \cdot \epsilon_{D^*}^*, \quad (33)$$

$$\mathcal{T}_4^i = \mathcal{U}_4 P_2^{ij,mn}\epsilon_{D^*}^{*m}\epsilon_{D^*}^{*n}(p_{D^*}^j - p_{D^*}^j). \quad (34)$$

Then the corresponding amplitudes squared are⁷

$$|\mathcal{M}_1|^2 = \mathcal{U}_1^2\frac{32\pi\alpha}{s}|p_D|^2(1 - \cos^2\theta), \quad (35)$$

$$|\mathcal{M}_2|^2 = \mathcal{U}_2^2\frac{32\pi\alpha}{s}|p_D|^2(1 + \cos^2\theta), \quad (36)$$

$$|\mathcal{M}_3|^2 = \mathcal{U}_3^2\frac{32\pi\alpha}{s}|p_{D^*}|^2(1 - \cos^2\theta), \quad (37)$$

$$|\mathcal{M}_4|^2 = \mathcal{U}_4^2\frac{112\pi\alpha}{5s}|p_{D^*}|^2(1 - \frac{1}{7}\cos^2\theta), \quad (38)$$

with the differential cross sections given by

$$\frac{d\sigma_i}{d\cos\theta} = \frac{|p_{D^{(*)}}|}{64\pi s^{3/2}}|\mathcal{M}_i|^2. \quad (39)$$

One can obtain the total cross section by integrating over the angle θ and then perform an overall fit to the $e^+e^- \rightarrow D\bar{D}$ [25], $D\bar{D}^*$ and $D^*\bar{D}^*$ [45] cross sections to extract the parameters of the model.

III. RESULTS AND DISCUSSIONS

In this section, we present our fit results and extract the interesting physical quantities which can be confirmed or excluded by further detailed energy scans at electron-positron colliders. To obtain the low-energy parameters (Table II), an overall fit to the $e^+e^- \rightarrow D\bar{D}$, $D\bar{D}^*$, and $D^*\bar{D}^*$ cross

⁷ The angular distribution has also been discussed in Ref. [44] for the bottomonium sector.

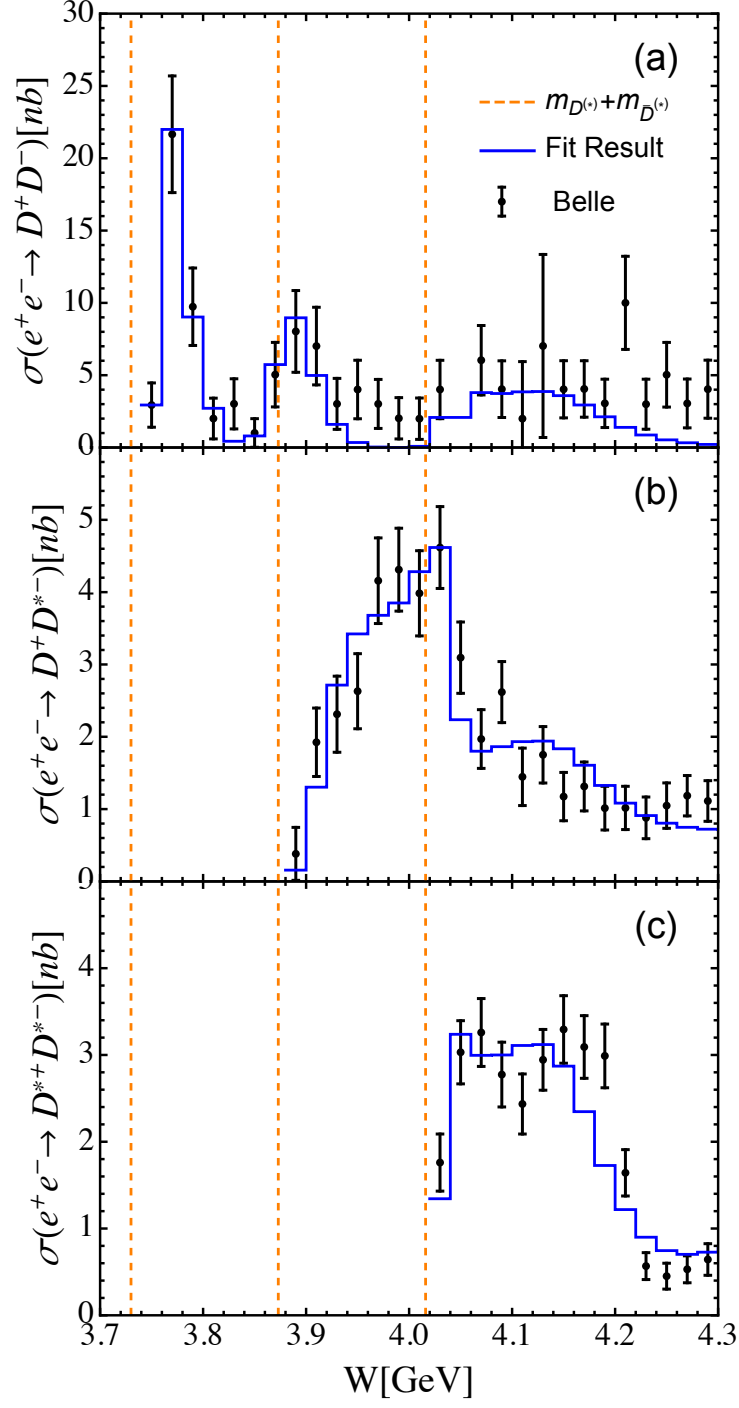


FIG. 2: The cross sections for $e^+e^- \rightarrow D^+D^-$, D^+D^{*-} , and $D^{*+}D^{*-}$ within the energy region [3.7, 4.25] GeV. The three vertical lines are the $D\bar{D}$, $D\bar{D}^*$, and $D^*\bar{D}^*$ thresholds, respectively. The experimental data are taken from the Belle Collaboration [25, 45].

TABLE II: The fit parameters.

$C_1(\text{GeV}^{-2})$	$C_2(\text{GeV}^{-2})$	$C_3(\text{GeV}^{-2})$	$C_4(\text{GeV}^{-2})$
79.70 ± 1.15	5.79 ± 0.22	43.90 ± 0.50	49.28 ± 1.37
$g_{2S}(\text{GeV}^0)$	$g_{3S}(\text{GeV}^0)$	$g_{1D}(\text{GeV}^0)$	$g_{2D}(\text{GeV}^0)$
0.90 ± 0.05	15.69 ± 0.04	3.65 ± 0.11	8.66 ± 0.15
$g_{2S}^0(\text{GeV}^2)$	$g_{3S}^0(\text{GeV}^2)$	$g_{1D}^0(\text{GeV}^2)$	$g_{2D}^0(\text{GeV}^2)$
0.22 ± 0.15	-0.17 ± 0.01	-0.05 ± 0.03	-0.15 ± 0.01
$f_S^0(\text{GeV}^0)$	$f_D^0(\text{GeV}^0)$	$a(3.9 \text{ GeV})$	$\chi^2/d.o.f.$
-1.55 ± 0.09	0.53 ± 0.08	0.56 ± 0.01	1.47

sections is carried out and the fit results are presented in Fig.2.⁸ In Table II the parameters C_i of the short-ranged contact interactions as defined in Eqs.(9) and (10) are displayed. Since C_2 reflects the contribution from $|1 \otimes 0\rangle$, which has the similar effect from the S -wave charmonia, some of its contribution could be absorbed into the nearby S -wave charmonia. The case for the parameter C_4 is analogous for the D -wave charmonia. The parameters g_{2S} , g_{3S} , g_{1D} , and g_{2D} are the bare couplings between the conventional $\psi(2S)$, $\psi(3S)$, $\psi(1D)$, $\psi(2D)$ and a pair of open charmed mesons. g_{2S}^0 , g_{3S}^0 , g_{1D}^0 , and g_{2D}^0 are the couplings between the $\psi(2S)$, $\psi(3S)$, $\psi(1D)$, $\psi(2D)$ and a virtual photon. Since g_{iS}^0 and g_{iD}^0 are the production strengths of S -wave and D -wave $c\bar{c}$ through a virtual photon, one can evaluate their ratio

$$\mathcal{R}_i \equiv \frac{g_{iD}^0}{g_{iS}^0} \sim \frac{(E - 2m_c)^2}{2(E + m_c)^2} \quad (40)$$

by plugging the plane wave Dirac spinors into the vector current $\bar{c}\gamma_\mu c$ with a $\mathcal{O}(\frac{\Lambda_{QCD}}{m_c})$ correction as discussed in Ref [46]. Here, E is the total energy and m_c is the charm quark mass. The ratio $\mathcal{R}_2 = 1.4\%$ is estimated with the energy at the average of $\psi(3686)$ and $\psi(4160)$ which are expected to be dominated by the $\psi(2S)$ and $\psi(2D)$ components, respectively. However, their fit values are at the same order which indicates that there are large corrections from higher order terms. f_S^0 and f_D^0 are the S -wave and D -wave components of the couplings between a virtual photon and a pair of charmed mesons. In principle, f_D^0/f_S^0 should be of the same order as \mathcal{R}_i defined in Eq.(40). However it could be largely modified by the final-state hadronic process[47], i.e. hadronizing to a pair of charmed mesons, which is not as good a quantity as \mathcal{R}_i to test higher order contributions.

A. The poles of $\psi(3770)$ and $\psi(4040)$

As shown in Fig.2, the signals of the expected charmonia $\psi(3770)$, $\psi(4040)$ and $\psi(4160)$ are very different in these three channels. The $\psi(3770)$ appears to be a pronounced peak which is isolated from other resonance structures. In comparison, the signals for both $\psi(4040)$ and $\psi(4160)$ are not significant in both $D\bar{D}$ and $D\bar{D}^*$ channels. They only show some structures in the $D^*\bar{D}^*$ channel. When the conventional charmonia are close to some thresholds, their mass positions, line shapes or other physical quantities can be largely influenced by their strong interactions with the open channels [48]. In general, the S -wave interactions will appear to be the most significant ones, but sometimes the P -wave will also become crucial as we will show in this work. To extract the resonance parameters of these charmonia and obtain a consistent understanding of the effect from the nearby thresholds, an overall fit within the coupled channel framework is necessary.

In the following, we extract the pole positions of the dressed charmonia on the complex energy plane. Since only poles which are located on the physical sheet or close ones can affect the physical

⁸ Here and in what follows, due to the status of the experimental data, theoretical uncertainties are not considered but left for the forthcoming work after including the one-pion exchange potential and the relevant three-body channels.

TABLE III: Poles on the sheets which are close to the physical sheet and the modules of the dimensionless couplings.

Sheet	Poles (GeV)	$ g_{D\bar{D}} $	$ g_{D\bar{D}^*} $	$ g_{D^*\bar{D}^*_{s=0}} $	$ g_{D^*\bar{D}^*_{s=2}} $
II	$3.764 \pm i0.006$	13.53	9.48	5.88	16.78
III	$3.879 \pm i0.035$	4.40	10.96	7.63	18.15
IV	$4.034 \pm i0.014$	2.90	2.23	12.52	12.85

measurement significantly, we only search for poles on these sheets. Accordingly, we only care about the poles in the following energy regions on each Riemann sheet,

$$\begin{aligned}
\text{I} \quad & \text{Im } q_{D\bar{D}} > 0, \quad \text{Im } q_{D\bar{D}^*} > 0, \quad \text{Im } q_{D^*\bar{D}^*} > 0, \quad \text{for } E < 2m_D, \\
\text{II} \quad & \text{Im } q_{D\bar{D}} < 0, \quad \text{Im } q_{D\bar{D}^*} > 0, \quad \text{Im } q_{D^*\bar{D}^*} > 0, \quad \text{for } 2m_D < E < m_D + m_{D^*}, \\
\text{III} \quad & \text{Im } q_{D\bar{D}} < 0, \quad \text{Im } q_{D\bar{D}^*} < 0, \quad \text{Im } q_{D^*\bar{D}^*} > 0, \quad \text{for } m_D + m_{D^*} < E < 2m_{D^*}, \\
\text{IV} \quad & \text{Im } q_{D\bar{D}} < 0, \quad \text{Im } q_{D\bar{D}^*} < 0, \quad \text{Im } q_{D^*\bar{D}^*} < 0, \quad \text{for } E > 2m_{D^*}.
\end{aligned}$$

As shown in Table III,⁹ the mass position of the $\psi(3770)$ on sheet II is 11 MeV lower than the measured mass 3773.15 ± 0.33 MeV, which is obtained by a Breit-Wigner fit. The fit width 12 MeV is much smaller than the measured width 27.2 ± 1.0 MeV. The deviation means that there are other decay modes for the $\psi(3770)$ as discussed in Ref.[49]. Another reason is that there is a difference between the pole width and the Breit-Wigner width for a broader state. The ratio of the effective couplings to the four channels is $13.53 : 9.48 : 5.88 : 16.78 = 1 : 0.70 : 0.43 : 1.24$ which is different from that of both a pure S -wave charmonium $\frac{1}{2\sqrt{3}} : \frac{1}{\sqrt{3}} : \frac{1}{6} : \frac{\sqrt{5}}{3} = 1 : 2 : 0.58 : 2.58$ and a pure

D -wave charmonium $\frac{1}{2}\sqrt{\frac{5}{3}} : \frac{1}{2}\sqrt{\frac{5}{3}} : \frac{\sqrt{5}}{6} : \frac{1}{6} = 1 : 1 : 0.58 : 0.26$. One might expect that the ratios should lie within the range limited by the values of the pure S -wave charmonium and pure D -wave charmonium. However, for instance, 0.70 is smaller than both 2 (S -wave case) and 1 (D -wave case). When the masses of D and D^* are set equal to each other, the ratios of the couplings lie between those of the pure S -wave charmonium and the pure D -wave charmonium as one expects. It indicates that the deviation is due to the HQSS breaking effects stemming from the mass splitting between D and D^* . Since it strongly couples to $D^*\bar{D}^*_{s=2}$ channel with the $|1 \otimes 0\rangle$ as the dominant component, the most important hidden charm decay channel is J/ψ plus two S -wave pions.¹⁰

We also find a pole $4.032 \pm i0.016$ GeV on sheet IV which corresponds to the $\psi(4040)$ with the ratio of the effective couplings $2.90 : 2.23 : 12.52 : 12.85 = 1 : 0.77 : 4.32 : 4.43$. It does not agree with either the ratio given by the pure S -wave or pure D -wave charmonia which also indicates large HQSS breaking effects. Since it couples to $D^*\bar{D}^*_{s=0}$ and $D^*\bar{D}^*_{s=2}$ channels which are dominated by the $|0 \otimes 1\rangle$ and $|1 \otimes 0\rangle$ components with relatively large strengths, respectively, its favored hidden charm decay channels would be η_c plus a light isosinglet vector (such as ω or three pions) and J/ψ plus two S -wave pions.

The poles corresponding to $\psi(3686)$ and $\psi(4160)$ are not listed in Table III. As the energy of $\psi(3686)$ is below the open charm thresholds, it mainly decays into light mesons and lower charmonia, in which case our method lacks precision. On the other side, $\psi(4160)$ is much more influenced by higher thresholds which we will investigate in detail in a forthcoming work.

⁹ One notices that the couplings in the table correspond to the relativistic fields. The non-relativistic ones can be obtained by dividing $\Pi_i \sqrt{2m_i}$ with m_i the masses of the heavy fields in the corresponding vertex.

¹⁰ PDG gives $\mathcal{BR}(\psi(3770) \rightarrow J/\psi \pi^+ \pi^-) = (1.93 \pm 0.28) \times 10^{-3}$ and $\mathcal{BR}(\psi(3770) \rightarrow J/\psi \pi^0 \pi^0) = (8.0 \pm 3.0) \times 10^{-4}$ which is larger than that of the other hidden charm decay channels.

B. The interpretation of the $G(3900)$

Since the observation of the $G(3900)$ in the ISR process $e^+e^- \rightarrow (\gamma)D\bar{D}$ by BABAR and Belle [24, 25] in 2007 and 2008, various groups have been paying attention to the P -wave interaction between a pair of charmed mesons [37, 39–42, 50]. The P -wave interaction between D and D^* is of great interest since it can be investigated in e^+e^- collisions. With the fit parameters, we find a pole at $3.879 \pm i0.032$ GeV on sheet III 4 MeV above the $D\bar{D}^*$ threshold, which corresponds to the $G(3900)$ structure. It is a resonance and can decay into the two lower channels, i.e. $D\bar{D}$ and $D\bar{D}^*$. Its coupling ratio to the four channels is $4.40 : 10.96 : 7.63 : 18.15 = 1 : 2.49 : 1.73 : 4.13$. Although it deviates from the ratios by the pure S -wave and pure D -wave charmonium, we cannot conclude that it does not have any $c\bar{c}$ component due to the HQSS breaking. Because it strongly couples to the $D\bar{D}^*$ and $D^*\bar{D}_{s=2}$ channels, it will show a significant threshold effect at the $D\bar{D}^*$ and $D^*\bar{D}^*$ thresholds, especially in the isospin breaking channels[51] due to the mass difference between the charged meson loops and the neutral ones. Since the $|1 \otimes 2\rangle$ and $|1 \otimes 0\rangle$ components dominate the $D\bar{D}^*$ and $D^*\bar{D}_{s=2}$ channels, respectively, we would also expect its signal in J/ψ plus two D -wave pions and S -wave pions channels. To further pin down the nature of the $G(3900)$, higher-statistics data are necessary.

C. The angular distribution in $D^*\bar{D}^*$ channels

As discussed in Sec. II A, the sum of the $D^*\bar{D}^*$ spins can either be zero or two for the $J^{PC} = 1^{--}$ channel. This corresponds to the angular distribution $1 - \cos^2 \theta$, Eq.(37), and $1 - \frac{1}{7} \cos^2 \theta$ [Eq. (38)], respectively. Since these two bases, i.e. the $D^*\bar{D}_{s=0}^*$ and $D^*\bar{D}_{s=2}^*$ bases, are orthogonal to each other, the events in the $D^*\bar{D}^*$ channel are the incoherent sum of these. The different angular distribution means that it can help to disentangle how large the $s = 0$ and $s = 2$ components should be and can also be viewed as evidence for our scenario.

Since the $1 - \frac{1}{7} \cos^2 \theta$ distribution cannot be distinguished from a flat distribution if the integrated luminosity is not high enough, one can alternatively define an asymmetry parameter

$$\mathcal{A}(E) \equiv \frac{\int_{-1.0}^{-0.5} \frac{d\sigma(E)}{d\cos\theta} d\cos\theta + \int_{0.5}^{1.0} \frac{d\sigma(E)}{d\cos\theta} d\cos\theta}{\sigma(E)} \quad (41)$$

to disentangle the components. As discussed above, since the $\psi(4160)$ will be affected by large effects from the next threshold, the angular distribution at 4.04 GeV is the best energy point to disentangle it. Our results indicate that the ratio between these two components at 4.04 GeV is

$$\frac{d\sigma_{s=0}/d\cos\theta}{d\sigma_{s=2}/d\cos\theta} = \frac{0.41(1 - \cos^2\theta)}{0.23(1 - \frac{1}{7}\cos^2\theta)}, \quad (42)$$

with the total cross sections 1.52 nb for $s = 0$ and 1.23 nb for $s = 2$. With our fit parameters, the asymmetry is estimated as

$$\mathcal{A}(4.04) = 0.39. \quad (43)$$

For pure $s = 0$ and pure $s = 2$, the asymmetries are $\mathcal{A}_{s=0}(4.04) = 0.31$ and $\mathcal{A}_{s=2}(4.04) = 0.48$, respectively. It can be confirmed or excluded by a further detailed energy scan at BESIII with high integrated luminosity.

D. Searching the 1^{-+} exotic candidate

Besides the 1^{--} quantum number for the P -wave interaction, 1^{-+} quantum number can also be obtained [52] as shown in Eqs. (7) and (8). Since 1^{-+} is an exotic quantum number which cannot be obtained with a conventional $c\bar{c}$ configuration, there is no bare charmonium pole contribution in this channel. The only relevant low-energy parameters are C_1 and C_3 due to the appearance

TABLE IV: Poles for the 1^{-+} channels on the physical sheet and the close sheets as well as their dimensionless couplings to each channel.

Sheets	Poles (GeV)	$ g_{D\bar{D}^*} $	$ g_{D^*\bar{D}^*_{s=1}} $
II	$3.915 \pm i0.003$	7.91	3.48

of the $|0 \otimes 1\rangle$ and $|1 \otimes 1\rangle$ components in the wave functions of the 1^{-+} channel. As a result, the corresponding contact potential is

$$V^{1^{-+}} = \begin{pmatrix} \frac{1}{2}C_1 + \frac{1}{2}C_3 & -\frac{1}{2}C_1 + \frac{1}{2}C_3 \\ -\frac{1}{2}C_1 + \frac{1}{2}C_3 & \frac{1}{2}C_1 + \frac{1}{2}C_3 \end{pmatrix}, \quad (44)$$

with the values of C_1 and C_3 given in Table II. Since the relevant channels are $D\bar{D}^*$ and $D^*\bar{D}^*$, we can define the physical Riemann sheets and the close sheets as

$$\begin{aligned} \text{I} \quad & \text{Im } q_{D\bar{D}^*} > 0, \quad \text{Im } q_{D^*\bar{D}^*} > 0, \quad \text{for } E < m_D + m_{D^*}, \\ \text{II} \quad & \text{Im } q_{D\bar{D}^*} < 0, \quad \text{Im } q_{D^*\bar{D}^*} > 0, \quad \text{for } m_D + m_{D^*} < E < 2m_{D^*}, \\ \text{III} \quad & \text{Im } q_{D\bar{D}^*} < 0, \quad \text{Im } q_{D^*\bar{D}^*} < 0, \quad \text{for } E > 2m_{D^*}. \end{aligned}$$

With the central values of C_1 and C_3 , we obtain two poles which would affect the measurements. One is on the physical sheet about 500 MeV below the $D\bar{D}^*$ threshold and couples to the $D\bar{D}^*$ and $D^*\bar{D}^*_{s=1}$ channels with equal strength. The equal couplings are a consequence of the two facts of the HQSS. One is that the two diagonal elements in the potential [Eq. (44)] are the same and similarly for those two off-diagonal elements. Another one is that the mass splitting between D and D^* is much smaller than the difference between the pole mass and the open-charm thresholds. In this case, the masses of D and D^* are approximately degenerate. No matter on which sheets the poles are located, once they are below the two thresholds (bound states on the physical sheet or virtual states on an unphysical sheet), they couple with equal strength to these two channels. However, since the pole is very deep with about 500 MeV binding energy, it is far beyond the applicable energy region of the contact term interaction. One cannot predict reliably any deep pole without energy-dependent potentials, such as the one-pion exchange potential.

We also find a pole $3.915 \pm i0.003$ GeV on sheet II with the effective couplings 7.91 and 3.48 to the $D\bar{D}^*$ and $D^*\bar{D}^*$ channels, respectively. It is only 40 MeV above the $D\bar{D}^*$ threshold which is acceptable with only the short-ranged contact interaction. The $|0 \otimes 1\rangle$ component has two possible S -wave decay channels dictated by the symmetry. The product can be either $h_c + (3\pi)_{1--}$ with the isosinglet $J^{PC} = 1^{--}$ three pions¹¹ or $\eta_c + (4\pi)_{1++}$. However, only the $\eta_c + (4\pi)_{1++}$ can be accessed due to the phase space constraint. The $|1 \otimes 1\rangle$ component can P -wave decay to both $J/\psi + (3\pi)_{1--}$ and $\chi_{cJ} + (2\pi)_{0++}$. Among those J/ψ plus three pions channel is the most favoured one due to its larger phase space. Therefore, we would expect that the $J/\psi + (3\pi)_{1--}$ and $\eta_c + (4\pi)_{1++}$ channels are the best ones to measure this potential 1^{-+} exotic state in the $e^+e^- \rightarrow \gamma J/\psi 3\pi$ and $e^+e^- \rightarrow \gamma \eta_c 4\pi$ processes.

The wave functions of the two 1^{-+} exotic states, i.e. Eqs.(7) and (8), are similar to those of the $Z_b(10610)$ and $Z_b(10650)$, cf. Eq. (3) in Ref. [53]. The similarity means that the signs of the component $|1 \times 1\rangle$ ($|0 \times 1\rangle$) with heavy quark spin $s_Q = 1$ ($s_Q = 0$) in these two wave functions are the same (opposite). Consequently, the production amplitudes of these two 1^{-+} states in $e^+e^- \rightarrow \gamma 1^{-+} \rightarrow \gamma J/\psi 3\pi$ and $e^+e^- \rightarrow \gamma 1^{-+} \rightarrow \gamma \eta_c 4\pi$ processes are

$$\mathcal{A}(e^+e^- \rightarrow \gamma 1^{-+} \rightarrow \gamma J/\psi 3\pi) \propto \frac{g_{\gamma 1} g_{J/\psi 1}}{E - E_1 + i\Gamma_1/2} + \frac{g_{\gamma 2} g_{J/\psi 2}}{E - E_2 + i\Gamma_2/2}, \quad (45)$$

$$\mathcal{A}(e^+e^- \rightarrow \gamma 1^{-+} \rightarrow \gamma \eta_c 4\pi) \propto \frac{g_{\gamma 1} g_{\eta_c 1}}{E - E_1 + i\Gamma_1/2} + \frac{g_{\gamma 2} g_{\eta_c 2}}{E - E_2 + i\Gamma_2/2}, \quad (46)$$

¹¹ Here and in what follows, the quantum number J^{PC} of pions are explicitly written as subindices.

with $g_{\gamma i}$ the coupling strengths between the i th 1^{-+} state and two photons. E_i and Γ_i are the energy and width of the i th 1^{-+} state, respectively. In the HQSS limit, $g_{J/\psi 2}/g_{J/\psi 1} = g_{\gamma 2}/g_{\gamma 1} = 1$ due to the same sign of the component $|1 \times 1\rangle$ in Eqs. (7) and (8). The case for the $|0 \times 1\rangle$ component is different, i.e. $g_{\eta_c 2}/g_{\eta_c 1} = -1$. One would expect that there is destructive (constructive) interference in the $J/\psi 3\pi$ ($\eta_c 4\pi$) invariant mass distribution when the energy lies between the pole positions, which is similar to that for the two Z_b states in the $\Upsilon\pi$ ($h_b\pi$) channel. However, the two poles in our case are not close enough to make this interference pattern as significant as that for the two Z_b states [53].

IV. SUMMARY

We have studied the P -wave $D\bar{D}$, $D\bar{D}^*$, and $D^*\bar{D}^*$ coupled channel effects with a the short-ranged separable contact term interaction in the heavy quark limit by solving the Lippmann-Schwinger equation. To extract the physical quantities, we fit the cross sections of $e^+e^- \rightarrow D\bar{D}$, $D\bar{D}^*$, and $D^*\bar{D}^*$ within the energy region [3.7, 4.25] GeV. Since there are some conventional charmonia, such as $\psi(2S)$, $\psi(3S)$, $\psi(1D)$, and $\psi(2D)$ in this mass region, these bare pole terms are also included in the calculation in addition to the contact potential. After having fitted the parameters of the model, we extract the pole positions of the $\psi(3770)$ and $\psi(4040)$ as well as their couplings to each channel. The pole positions of both $\psi(3686)$ and $\psi(4160)$ are left for the forthcoming work after including all the relevant thresholds. It is an efficient and consistent way to extract the resonance parameters and the couplings of a state below threshold. Besides the two poles, another pole at $3.879 \pm i0.035$ GeV on the unphysical sheet is also found which may correspond to the so-called $G(3900)$ observed by BABAR and Belle. However, due to the limitations in statistics of these data, to further pin down the nature of $G(3900)$ a detailed scan of the open charmed channels in the e^+e^- annihilation process is necessary. We also propose that the angular distribution, or the asymmetry \mathcal{A} if the luminosity is not high enough, in the $D^*\bar{D}^*$ channel can test our model.

Besides the 1^{-+} quantum number, the P -wave $D\bar{D}^*$ and $D^*\bar{D}^*$ interaction can also access the exotic 1^{-+} quantum number. Since 1^{-+} is an exotic quantum number, there is no bare pole term in this channel. With the relevant parameters C_1 and C_3 fitted in the 1^{--} channels, we find a pole $3.915 \pm i0.003$ GeV, 40MeV above $D\bar{D}^*$ threshold. It can be measured in the $J/\psi + 3\pi$ and $\eta_c + 4\pi$ invariant mass distributions in $e^+e^- \rightarrow \gamma J/\psi 3\pi$ and $e^+e^- \rightarrow \gamma \eta_c 4\pi$ processes by further experiments with high integrated luminosity.

ACKNOWLEDGMENTS

We give thanks to Feng-Kun Guo, Zhi-Hui Guo, Christoph Hanhart, and Qiang Zhao for useful discussions and comments. This work is supported in part by the DFG and the NSFC through funds provided to the Sino-German CRC 110 ‘‘Symmetries and the Emergence of Structure in QCD.’’ The work of U. G. M. was also supported by the Chinese Academy of Sciences (CAS) President’s International Fellowship Initiative (PIFI) (Grant No. 2015VMA076).

Appendix A: THE EFFECTIVE LAGRANGIAN OF S -WAVE AND D -WAVE CHARMONIA COUPLING TO A PAIR OF CHARMED MESONS

Due to the heavy quark spin symmetry, the S -wave charmed mesons, i.e. D and D^* , can be collected as a spin doublet superfield $H_a = V_a^i \sigma^i + P_a$ which annihilates the corresponding $Q\bar{q}$ charmed mesons. Here, V and P denote vector and pseudoscalar charmed mesons, respectively. Its charged conjugate partner is $\bar{H}_a = \sigma_2 \mathcal{C} H_a^T \mathcal{C}^{-1} \sigma_2 = -\bar{V}_a^i \sigma^i + \bar{P}_a$ with the convention $\mathcal{C} V \mathcal{C}^{-1} = \bar{V}$ and $\mathcal{C} P \mathcal{C}^{-1} = \bar{P}$. The corresponding creation superfield is

$$H_a^\dagger = V_a^{i\dagger} \sigma^i + P_a^\dagger, \quad \bar{H}_a^\dagger = -\bar{V}_a^{i\dagger} \sigma^i + \bar{P}_a^\dagger. \quad (\text{A1})$$

In the heavy quark limit, the S -wave and D -wave charmonia can also be collected in multiplets $J = \psi^i \sigma^i + \dots$ and

$$J^{ij} = \frac{1}{2} \sqrt{\frac{3}{5}} (\sigma^i \psi_{D1}^j + \sigma^j \psi_{D1}^i) - \frac{1}{\sqrt{15}} \delta^{ij} \vec{\sigma} \cdot \vec{\psi}_{D1} + \dots \quad (\text{A2})$$

Since we consider the 1^{--} channel, only the relevant vector charmonia are presented explicitly. The Lagrangian of the S -wave and D -wave charmonia coupling to a pair of charmed mesons reads

$$\mathcal{L} = i \frac{g_S}{2} \langle J^\dagger H_a \sigma^i \overleftrightarrow{\partial}^i \bar{H}_a \rangle + i \frac{g_D}{2} \langle J^{ij\dagger} H_a \sigma^i \overleftrightarrow{\partial}^j \bar{H}_a \rangle + \text{H.c.} \quad (\text{A3})$$

with the overall coupling strength g_S and g_D . Using the above interaction, one can also get the same branching ratio fractions as shown in Table I.

Appendix B: LOOP FUNCTIONS

In this appendix, we present the relevant one-loop integrals explicitly. We use the standard tensor reduction [54] to express the occurring integrals as a linear sum of scalar one-loop functions. Here we only present the one-loop function we need in the calculation [55]. The other two-point one-loop functions can be found in Ref.[55].

We use

$$R = \frac{2}{d-4} + \gamma_E - \ln(4\pi), \quad (\text{B1})$$

to denote the ultraviolet divergences with γ_E the Euler constant and d the number of space-time dimensions. The one-point function is defined as

$$\mathcal{I}_0(M_a^2) = \frac{\mu^{4-d}}{i} \int \frac{d^d k}{(2\pi)^d} \frac{1}{k^2 - M_a^2 + i0^+} = -\frac{M_a^2}{16\pi^2} \left(R - 1 + \ln \frac{M_a^2}{\mu^2} \right). \quad (\text{B2})$$

The second rank tensor loop can be decomposed as

$$\begin{aligned} \mathcal{G}^{\mu\nu}(p^2, M_a^2, M_b^2) &= \frac{\mu^{4-d}}{i} \int \frac{d^d k}{(2\pi)^d} \frac{k^\mu k^\nu}{(k^2 - M_a^2 + i0^+) [(k+p)^2 - M_b^2 + i0^+]} \\ &= g^{\mu\nu} \mathcal{G}_{00}(p^2, M_a^2, M_b^2) + p^\mu p^\nu \mathcal{G}_{11}(p^2, M_a^2, M_b^2), \end{aligned} \quad (\text{B3})$$

where

$$\begin{aligned} \mathcal{G}_{00}(p^2, M_a^2, M_b^2) &= \frac{1}{12p^2} ((p^2 + \Delta_{ab}) \mathcal{I}_0(M_a^2) + (p^2 - \Delta_{ab}) \mathcal{I}_0(M_b^2)) \\ &\quad + [4p^2 M_a^2 - (p^2 + \Delta_{ab})^2] \mathcal{G}(p^2, M_a^2, M_b^2) - \frac{1}{16\pi^2} \frac{1}{18} (p^2 - 3\Sigma_{ab}), \end{aligned}$$

with $\Delta_{ab} \equiv M_a^2 - M_b^2$ and $\Sigma_{ab} \equiv M_a^2 + M_b^2$. In the heavy quark symmetry limit, i.e. $m_D = m_{D^*}$, the $\mathcal{I}_0(M^2)$ part would be a constant which could be absorbed into the contact terms C_i . Further, the fundamental loop integral $\mathcal{G}(s, M_a^2, M_b^2)$ reads

$$\mathcal{G}(s, M_a^2, M_b^2) = \frac{1}{16\pi^2} \left\{ a(\mu) - \ln \frac{M_a^2}{\mu^2} - \frac{s - M_a^2 + M_b^2}{2s} \ln \frac{M_b^2}{M_a^2} \right. \quad (\text{B4})$$

$$\left. - \frac{\sigma_{ab}}{2s} [\ln(s - M_b^2 + M_a^2 + \sigma_{ab}) - \ln(-s + M_b^2 - M_a^2 + \sigma_{ab})] \right. \quad (\text{B5})$$

$$\left. + \ln(s + M_b^2 - M_a^2 + \sigma_{ab}) - \ln(-s - M_b^2 + M_a^2 + \sigma_{ab}) \right\} \quad (\text{B6})$$

with $\sigma_{ab} = \sqrt{[s - (M_a + M_b)^2][s - (M_a - M_b)^2]}$ and $a(\mu)$ the subtraction constant which depends on the scale of dimensional regularization μ .

- [2] N. A. Tornqvist, Phys. Lett. B **590**, 209 (2004) [hep-ph/0402237].
- [3] N. A. Tornqvist, Phys. Rev. Lett. **67**, 556 (1991).
- [4] E. S. Swanson, Phys. Lett. B **588**, 189 (2004) [hep-ph/0311229].
- [5] E. Braaten, M. Lu and J. Lee, Phys. Rev. D **76**, 054010 (2007) [hep-ph/0702128 [HEP-PH]].
- [6] S. Fleming, M. Kusunoki, T. Mehen and U. van Kolck, Phys. Rev. D **76**, 034006 (2007) [hep-ph/0703168].
- [7] P. Wang and X. G. Wang, Phys. Rev. Lett. **111**, no. 4, 042002 (2013) [arXiv:1304.0846 [hep-ph]].
- [8] V. Baru, E. Epelbaum, A. A. Filin, F.-K. Guo, H.-W. Hammer, C. Hanhart, U.-G. Meißner and A. V. Nefediev, Phys. Rev. D **91**, no. 3, 034002 (2015) [arXiv:1501.02924 [hep-ph]].
- [9] V. Baru, A. A. Filin, C. Hanhart, Y. S. Kalashnikova, A. E. Kudryavtsev and A. V. Nefediev, Phys. Rev. D **84**, 074029 (2011) [arXiv:1108.5644 [hep-ph]].
- [10] Y. Chen *et al.*, Phys. Rev. D **89**, no. 9, 094506 (2014) [arXiv:1403.1318 [hep-lat]].
- [11] J. He, Phys. Rev. D **90**, no. 7, 076008 (2014) [arXiv:1409.8506 [hep-ph]].
- [12] S. Coito, Phys. Rev. D **94**, no. 1, 014016 (2016) [arXiv:1602.07821 [hep-ph]].
- [13] L. Zhao, L. Ma and S. L. Zhu, Nucl. Phys. A **942**, 18 (2015) [arXiv:1504.04117 [hep-ph]].
- [14] Y. Chen *et al.* [CLQCD Collaboration], Phys. Rev. D **92**, no. 5, 054507 (2015) [arXiv:1503.02371 [hep-lat]].
- [15] S. Prelovsek, C. B. Lang, L. Leskovec and D. Mohler, Phys. Rev. D **91**, no. 1, 014504 (2015) [arXiv:1405.7623 [hep-lat]].
- [16] F. Aceti, M. Bayar, E. Oset, A. Martinez Torres, K. P. Khemchandani, J. M. Dias, F. S. Navarra and M. Nielsen, Phys. Rev. D **90**, no. 1, 016003 (2014) [arXiv:1401.8216 [hep-ph]].
- [17] F. Aceti, M. Bayar, J. M. Dias and E. Oset, Eur. Phys. J. A **50**, 103 (2014) [arXiv:1401.2076 [hep-ph]].
- [18] F. K. Guo, C. Hidalgo-Duque, J. Nieves and M. P. Valderrama, Phys. Rev. D **88**, 054007 (2013) [arXiv:1303.6608 [hep-ph]].
- [19] J. M. Dias, F. Aceti and E. Oset, Phys. Rev. D **91**, no. 7, 076001 (2015) [arXiv:1410.1785 [hep-ph]].
- [20] Z. F. Sun, J. He, X. Liu, Z. G. Luo and S. L. Zhu, Phys. Rev. D **84**, 054002 (2011) [arXiv:1106.2968 [hep-ph]].
- [21] M. Cleven, F. K. Guo, C. Hanhart and U.-G. Meißner, Eur. Phys. J. A **47**, 120 (2011) [arXiv:1107.0254 [hep-ph]].
- [22] C. Hanhart, Y. S. Kalashnikova, P. Matuschek, R. V. Mizuk, A. V. Nefediev and Q. Wang, Phys. Rev. Lett. **115**, no. 20, 202001 (2015) [arXiv:1507.00382 [hep-ph]].
- [23] F.-K. Guo, C. Hanhart, Y. S. Kalashnikova, P. Matuschek, R. V. Mizuk, A. V. Nefediev, Q. Wang and J.-L. Wynn, Phys. Rev. D **93**, no. 7, 074031 (2016) [arXiv:1602.00940 [hep-ph]].
- [24] B. Aubert *et al.* [BaBar Collaboration], Phys. Rev. D **76**, 111105 (2007) [hep-ex/0607083].
- [25] G. Pakhlova *et al.* [Belle Collaboration], Phys. Rev. D **77**, 011103 (2008) [arXiv:0708.0082 [hep-ex]].
- [26] C. Z. Yuan *et al.* [Belle Collaboration], Phys. Rev. Lett. **99**, 182004 (2007) [arXiv:0707.2541 [hep-ex]].
- [27] B. Aubert *et al.* [BaBar Collaboration], Phys. Rev. Lett. **95**, 142001 (2005) [hep-ex/0506081].
- [28] B. Aubert *et al.* [BaBar Collaboration], Phys. Rev. Lett. **98**, 212001 (2007) [hep-ex/0610057].
- [29] G. Pakhlova *et al.* [Belle Collaboration], Phys. Rev. Lett. **101**, 172001 (2008) [arXiv:0807.4458 [hep-ex]].
- [30] X. L. Wang *et al.* [Belle Collaboration], Phys. Rev. Lett. **99**, 142002 (2007) [arXiv:0707.3699 [hep-ex]].
- [31] Z. Q. Liu, X. S. Qin and C. Z. Yuan, Phys. Rev. D **78**, 014032 (2008) [arXiv:0805.3560 [hep-ex]].
- [32] A. E. Bondar and M. B. Voloshin, Phys. Rev. D **93**, no. 9, 094008 (2016) [arXiv:1603.08436 [hep-ph]].
- [33] X. H. Liu, Phys. Rev. D **90**, no. 7, 074004 (2014) [arXiv:1403.2818 [hep-ph]].
- [34] M. Cleven, Q. Wang, F. K. Guo, C. Hanhart, U.-G. Meißner and Q. Zhao, Phys. Rev. D **90**, no. 7, 074039 (2014) [arXiv:1310.2190 [hep-ph]].
- [35] W. Qin, S. R. Xue and Q. Zhao, arXiv:1605.02407 [hep-ph].
- [36] S. Dubynskiy and M. B. Voloshin, Phys. Rev. D **74**, 094017 (2006) [hep-ph/0609302].
- [37] Y. J. Zhang and Q. Zhao, Phys. Rev. D **81**, 074016 (2010) [arXiv:1002.1612 [hep-ph]].
- [38] F. K. Guo, C. Hanhart, G. Li, U.-G. Meißner and Q. Zhao, Phys. Rev. D **83**, 034013 (2011) [arXiv:1008.3632 [hep-ph]].
- [39] G. Y. Chen and Q. Zhao, Phys. Lett. B **718**, 1369 (2013) [arXiv:1209.6268 [hep-ph]].
- [40] Y. R. Liu, M. Oka, M. Takizawa, X. Liu, W. Z. Deng and S. L. Zhu, Phys. Rev. D **82**, 014011 (2010) [arXiv:1005.2262 [hep-ph]].
- [41] N. N. Achasov and G. N. Shestakov, Phys. Rev. D **86**, 114013 (2012) [arXiv:1208.4240 [hep-ph]].
- [42] X. Cao and H. Lenske, arXiv:1410.1375 [nucl-th].
- [43] G. Pakhlova *et al.* [Belle Collaboration], Phys. Rev. D **83**, 011101 (2011) [arXiv:1011.4397 [hep-ex]].
- [44] M. B. Voloshin, Phys. Rev. D **85**, 034024 (2012) [arXiv:1201.1222 [hep-ph]].
- [45] G. Pakhlova *et al.* [Belle Collaboration], Phys. Rev. Lett. **98**, 092001 (2007) [hep-ex/0608018].
- [46] X. Li and M. B. Voloshin, Phys. Rev. D **88**, no. 3, 034012 (2013) [arXiv:1307.1072 [hep-ph]].
- [47] Q. Wang, M. Cleven, F. K. Guo, C. Hanhart, U. G. Meißner, X. G. Wu and Q. Zhao, Phys. Rev. D **89**,

- no. 3, 034001 (2014) [arXiv:1309.4303 [hep-ph]].
- [48] E. J. Eichten, K. Lane and C. Quigg, Phys. Rev. D **73**, 014014 (2006) Erratum: [Phys. Rev. D **73**, 079903 (2006)] [hep-ph/0511179].
 - [49] Y. J. Zhang, G. Li and Q. Zhao, Phys. Rev. Lett. **102**, 172001 (2009) [arXiv:0902.1300 [hep-ph]].
 - [50] E. Eichten, K. Gottfried, T. Kinoshita, K. D. Lane and T. M. Yan, Phys. Rev. D **21**, 203 (1980).
 - [51] Q. Wang, X. H. Liu and Q. Zhao, Phys. Rev. D **84**, 014007 (2011) [arXiv:1103.1095 [hep-ph]].
 - [52] Q. Wang, Phys. Rev. D **89**, no. 11, 114013 (2014) [arXiv:1403.2243 [hep-ph]].
 - [53] A. E. Bondar, A. Garmash, A. I. Milstein, R. Mizuk and M. B. Voloshin, Phys. Rev. D **84**, 054010 (2011) [arXiv:1105.4473 [hep-ph]].
 - [54] G. Passarino and M. J. G. Veltman, Nucl. Phys. B **160**, 151 (1979).
 - [55] D. L. Yao, M. L. Du, F. K. Guo and U.-G. Meißner, JHEP **1511**, 058 (2015) [arXiv:1502.05981 [hep-ph]].